*Original*

Rao, K.P.; Prasad, Y.V.R.K.; Hort, N.; Kainer, K.U.:

**High Temperature Deformation Mechanisms and Processing Map for Hot Working of Cast-Homogenized Mg-3Sn-2Ca Alloy**

In: Materials Science Forum, THERMEC 2009 (2010) Trans Tech Publications

DOI: 10.4028/www.scientific.net/MSF.638-642.3616

*Materials Science Forum* *Online: 2010-01-12*
*ISSN: 1662-9752, Vols. 638-642, pp 3616-3621*
*doi:10.4028/www.scientific.net/MSF.638-642.3616*


# High Temperature Deformation Mechanisms and Processing Map for Hot Working of Cast-Homogenized Mg-3Sn-2Ca Alloy

K.P. Rao[1, a], Y.V.R.K. Prasad[1, b], N. Hort[2, c] and K.U. Kainer[2, d]

[1]Department of Manufacturing Engineering and Engineering Management
City University of Hong Kong, 83 Tat Chee Avenue Kowloon, Hong Kong SAR, China

[2]GKSS Research Centre Geesthacht GmbH, Max-Planck Str. 1, Geesthact 21502, Germany

[a]mekprao@cityu.edu.hk, [b]meprasad@cityu.edu.hk, [c]norbert.hort@gkss.de, [d]kainer@gkss.de

**Keywords:** Mg-Sn-Ca Alloy, Hot Workability, Processing Map, Kinetic Analysis, Dynamic Recrystallization

**Abstract.** The hot working behavior of Mg-3Sn-2Ca alloy has been investigated in the temperature range 300–500 $^{o}$C and strain rate range 0.0003–10 $s^{-1}$, with a view to evaluate the mechanisms and optimum parameters of hot working. For this purpose, a processing map has been developed on the basis of the flow stress data obtained from compression tests. The stress-strain curves exhibited steady state behavior at strain rates lower than 0.01 $s^{-1}$ and at temperatures higher than 350 $^{o}$C and flow softening occurred at higher strain rates. The processing map exhibited two dynamic recrystallization domains in the temperature and strain rate ranges: (1) 300–420 $^{o}$C and 0.0003–0.003 $s^{-1}$, and (2) 420–500 $^{o}$C and 0.003–1.0 $s^{-1}$, the latter one being useful for commercial hot working. Kinetic analysis yielded apparent activation energy values of 161 and 175 kJ/mole in domains (1) and (2) respectively. These values are higher than that for self-diffusion in magnesium suggesting that the large volume fraction of intermetallic particles CaMgSn present in the matrix generates considerable back stress. The processing map reveals a wide regime of flow instability which gets reduced with increase in temperature or decrease in strain rate.

## Introduction

Mg-Sn-Ca alloys (TX series) are newer wrought alloys that are designed to possess corrosion and creep resistance [1-3]. In this system, Sn forms solid solution with Mg and imparts corrosion resistance while Ca forms intermetallic particles in the matrix that enhance high temperature creep resistance of the alloy. Among the several compositions being considered, Mg-3Sn-2Ca alloy (TX32) is identified to be the most promising since it offers better creep resistance than the commonly recommended alloy AE42 and AZ91 [3,4]. The microstructure of TX32 revealed [3] the presence of the intermetallic particles of CaMgSn mostly in the matrix and $Mg_2Ca$ phase at the grain boundaries, both of which are beneficial in enhancing the creep resistance of the alloy. Preliminary studies of the hot workability of TX32 indicated that the alloy can be extruded to obtain a fine grained recrystallized microstructure [4]. The aim of the present investigation is to evaluate in detail the hot working behavior of TX32 with a view to obtain the optimum processing parameters and to establish the mechanisms of hot deformation.

The hot working behavior has been characterized using processing maps as well as the standard kinetic approach. The technique of processing maps is based on the dynamic materials model, the principles of which are described earlier [5-7]. Briefly, the work-piece undergoing hot deformation is considered to be a dissipator of power and the strain rate sensitivity ($m$) of flow stress is the factor that partitions power between deformation heat and microstructural changes. The efficiency of power dissipation occurring through microstructural changes during deformation ($\eta$) is derived by comparing the non-linear power dissipation occurring instantaneously in the work-piece with that of a linear dissipater for which the $m$ value is unity, and is given by:

$$\eta = 2m/(m+1). \quad (1)$$

The variation of efficiency of power dissipation with temperature and strain rate represents a *power dissipation map* which is generally viewed as an iso-efficiency contour map. Further, the extremum principles of irreversible thermodynamics as applied to continuum mechanics of large plastic flow [8] are explored to define a criterion for the onset of flow instability given by the equation for the instability parameter $\xi(\dot{\varepsilon})$:

$$\xi(\dot{\varepsilon}) = \frac{\partial \ln[m/(m+1)]}{\partial \ln \dot{\varepsilon}} + m \leq 0 . \quad (2)$$

The variation of the instability parameter as a function of temperature and strain rate represents an *instability map* which delineates regimes of instability where $\xi$ is negative. A superimposition of the instability map on the power dissipation map gives a *processing map* which reveals *domains* (efficiency contours converging towards a peak efficiency) where individual microstructural processes dominate and the limiting conditions for the *regimes* (bounded by a contour for $\xi = 0$) of flow instability. Processing maps help in identifying temperature – strain rate windows for hot working where the intrinsic workability of the material is maximum (e.g. dynamic recrystallization (DRX) or superplasticity) and also in avoiding the regimes of flow instabilities (e.g. adiabatic shear bands or flow localization).

The standard kinetic rate equation relating the steady state flow stress ($\sigma$) to strain rate ($\dot{\varepsilon}$) and temperature ($T$) is given by [9]:

$$\dot{\varepsilon} = A\sigma^n \exp\left[-\frac{Q}{RT}\right] \quad (3)$$

where $A$ = constant, $n$ = stress exponent, $Q$ = activation energy, and $R$ = gas constant. The rate-controlling mechanisms are identified on the basis of the activation parameters $n$ and $Q$.

## Experimental

Mg – 3 wt.% Sn – 2 wt.% Ca alloy was prepared using 99.99% pure Mg, 99.96% pure Sn and 98.5% pure Ca. The alloy, molten at about 720 $^{o}$C, was kept under a protective cover of Ar+3% $SF_6$ gas before casting in a pre-heated permanent mold to obtain cylindrical billets of 100 mm diameter and 350 mm length. The billets were homogenized at 475 $^{o}$C for 5 hours and furnace cooled.

Cylindrical specimens of 9.8 mm diameter and 15 mm height were machined from the cast-homogenized billet for compression testing. For inserting a thermocouple to measure the specimen temperature as well as the adiabatic temperature rise during deformation, the specimens were provided with a 0.8 mm diameter hole machined at mid height to reach the centre of the specimen.

Isothermal uniaxial compression tests were conducted at constant true strain rates in the range 0.0003–10 $s^{-1}$ and temperature range 300–500 $^{o}$C. Details of the test set-up and procedure are described in earlier publication [10]. Constant true strain rates during the tests were achieved using an exponential decay of actuator speed in the servo hydraulic machine. Graphite powder mixed with grease was used as the lubricant in all the experiments. The specimens were deformed up to a true strain of 0.7 and then quenched in water. The load – stroke data were converted into true stress – true strain curves using standard equations. The flow stress values were corrected for the adiabatic temperature rise. Processing maps were developed using the procedures described earlier [5] and with the flow stress data at different temperatures, strain rates and strains obtained from the above experiments as in-puts. The deformed specimens were sectioned in the center parallel to the compression axis and the cut surface was mounted, polished and etched for metallographic examination. All the specimens were etched with an aqueous solution containing 10% picric acid.

## Results and Discussion

The microstructure of the starting material in cast-homogenized condition is shown in Fig. 1(a). The grain size was large (average grain diameter was about 700 μm) and the microstructure was dendritic. The scanning electron micrograph of the alloy is shown in Fig. 1(b) and EDS

analysis revealed the presence of CaMgSn and $Mg_2Ca$ phases.

The true stress – true strain curves obtained at the test temperatures of 300 $^oC$ and 500 $^oC$ are shown in Fig. 2. At strain rates higher than about 0.01 $s^{-1}$, the flow stress rapidly increased with increasing strain and reached a peak value before flow softening occurred. At lower strain rates, the flow curves exhibited near steady state deformation.

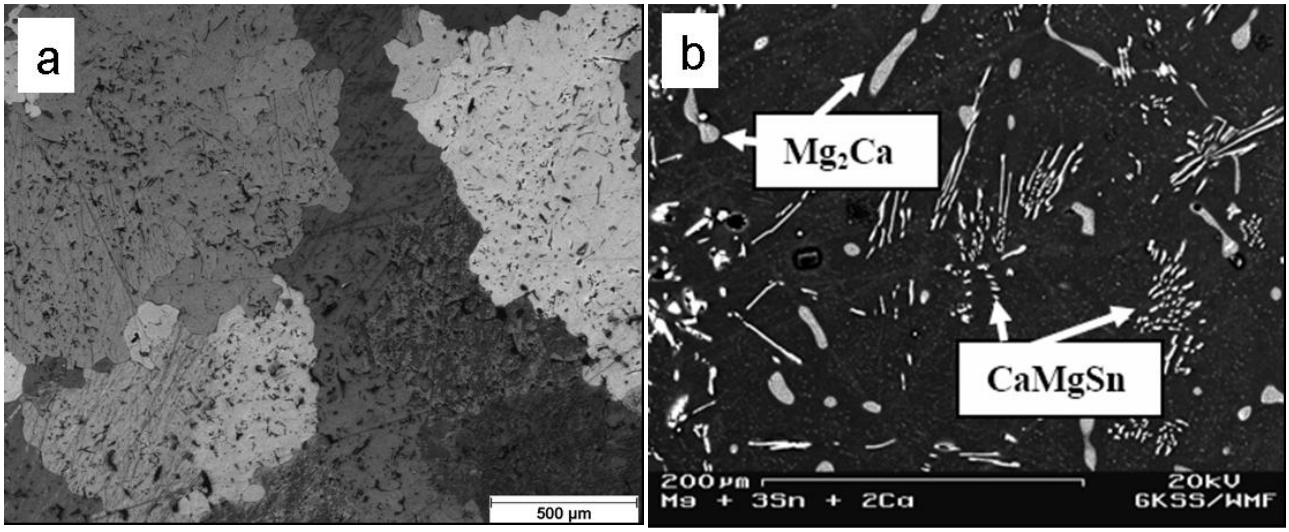


Fig. 1. (a) Optical and (b) Scanning electron micrographs of cast-homogenized TX32 alloy, the latter showing CaMgSn and $Mg_2Ca$ phases.

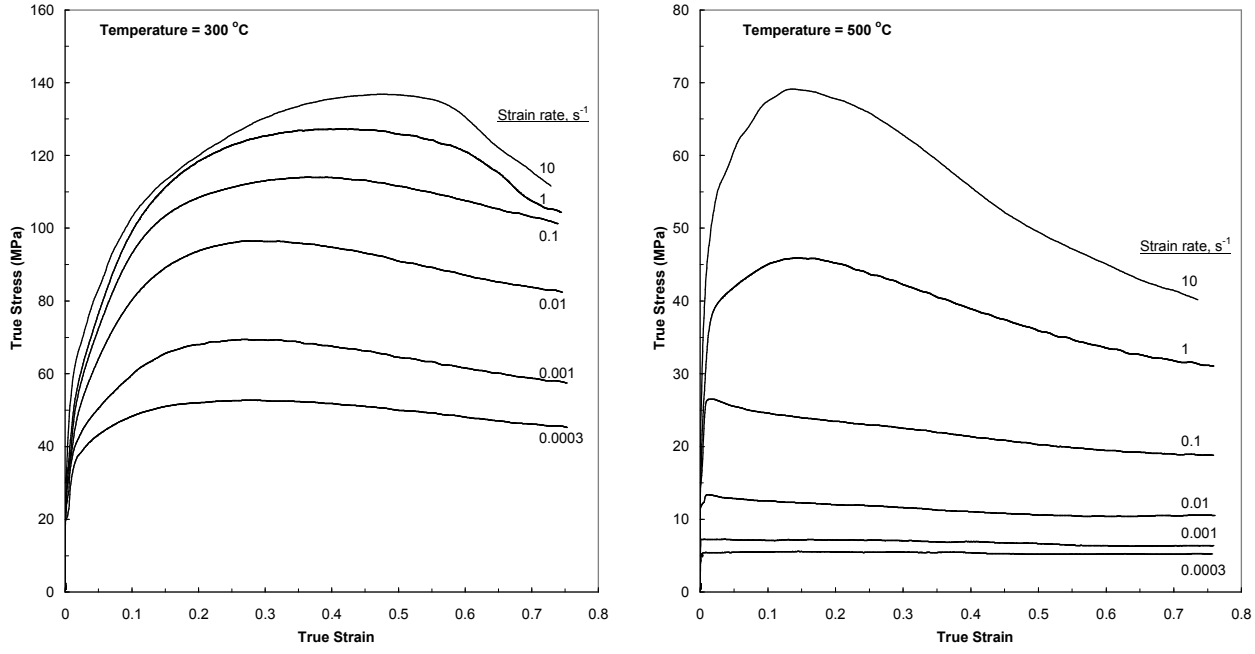


Fig. 2. True stress – true strain curves obtained on TX32 alloy in compression at different strain rates and at the test temperature of 300 $^oC$ and 500 $^oC$.

The processing map obtained at a strain of 0.5 (near steady state flow) is shown in Fig. 3, which exhibits two domains in the temperature and strain rate ranges: (1) 300–420 $^oC$ and 0.0003–0.003 $s^{-1}$, and (2) 420–500 $^oC$ and 0.003–1.0 $s^{-1}$. These domains have similar peak efficiency values (44 and 43%) which occur at (1) 360 $^oC$/0.0003 $s^{-1}$ and (2) 500 $^oC$/0.1 $s^{-1}$, respectively. The domains are separated at a temperature of about 420 $^oC$ with an energy saddle configuration, which might have been caused by a change in the rate controlling process triggered when a significant amount of calcium (≥1 wt.%) gets partitioned to Mg matrix beyond about 400 $^oC$ to form a solid solution. Hot extrusion of the alloy at 350$^oC$ has resulted in a uniform and finely recrystallized microstructure in

the product as shown in Fig. 4, indicating that dynamic recrystallization has occurred. The processing map has revealed a regime of flow instability, which is wider at lower temperatures (<420 $^{o}$C) and higher strain rates.

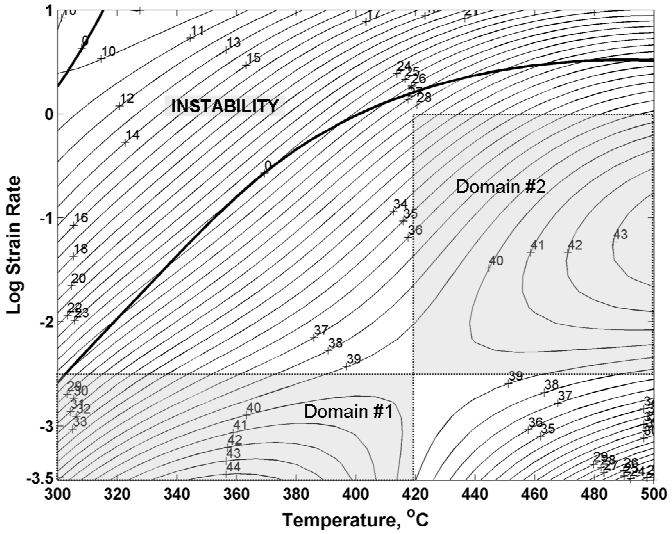


Fig. 3. Processing map for TX32 alloy obtained at a strain of 0.5. The numbers against the contours represent percent efficiency and the area above the dark like indicates flow instability.

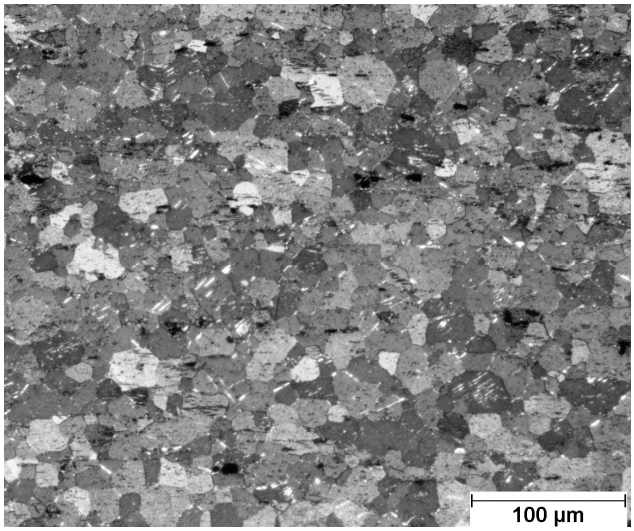


Fig. 4. Polarized light micrograph of the extruded TX32 alloy. The extrusion direction is horizontal.

Using the standard kinetic rate equation (Eq. 3) to represent the steady-state flow under hot working conditions [9], the activation parameters – stress exponent ($n$) and apparent activation energy ($Q$) – are evaluated. It may be noted that Eq. 3 is obeyed in the deterministic domains of the map. A plot of log(flow stress) versus log(strain rate) at different test temperatures, is shown in Fig. 5(a). All the data at the temperature of 500 $^{o}$C exhibited a good linear fit with a slope ($m$) of 0.26 or stress exponent ($n$) of 3.85. With decreasing temperatures up to 350 $^{o}$C, the linear fit got progressively limited to lower strain rates. The data for 300 $^{o}$C shows deviations since it falls outside the domain. At higher strain rates where the rate equation (Eq. 3) is not obeyed, the processing map exhibited flow instability regime. Arrhenius plot relating normalized flow stress [log ($\sigma/\mu$)] to ($1/T$) ($\mu$ = shear modulus) is shown in Fig. 5(b). The data at strain rates of 0.0003 $s^{-1}$ and 0.001 $s^{-1}$, which belong to Domain #1 of the processing map, exhibited a linear fit giving an apparent activation energy of 161 kJ/mole. On the other hand, the data at strain rates of 0.01 $s^{-1}$ and 0.1 $s^{-1}$, which belong to Domain #2 of the processing map, gave a linear fit only at higher temperatures and yielded an apparent activation energy of 175 kJ/mole. At strain rates of 1.0 $s^{-1}$ and 10 $s^{-1}$, the data did not obey the rate equation since it does not belong to any deterministic domain but fall in the flow instability regime.

The apparent activation energy values obtained in the two domains of the map are larger than that for lattice self diffusion in Mg (135 kJ/mole) [11]. This could be due to the large back stress generated by the large volume fraction of CaMgSn intermetallic particles in the matrix. While this can be comprehended in relation to Domain #1 occurring at lower strain rates, the intriguing result is that of Domain #2 occurring at higher strain rates (>0.01 $s^{-1}$). In other magnesium alloys like AZ31(Mg-3Al-1Zn) and TX31 (Mg-3Sn-1Ca), the processing maps exhibited a higher strain rate domain in which the apparent activation energy is *lower* than that for lattice self-diffusion and near that for grain boundary self diffusion [12-16]. In fact, this domain is the recommended one for processing these alloys since the strain rates correspond to those that can be easily obtained in commercial processes like rolling and extrusion. The difference in the behavior of TX32 may be attributed to the presence of $Mg_2Ca$ precipitates at the grain boundaries of its microstructure. This

has two effects on the mechanical behavior depending upon the strain rate: (1) At lower strain rates, $Mg_2Ca$ at grain boundaries reduces grain boundary sliding and reduces the creep rate. (2) At higher strain rates, $Mg_2Ca$ phase at grain boundaries may reduce the grain-boundary self-diffusion. Alternately, it is possible that other recovery mechanisms like cross-slip may be occurring in the second domain since at temperatures higher than 400°C, pyramidal slip will be contributing extensively to deformation. The stacking fault energy on the second order pyramidal systems is estimated to be about 173 mJ/m$^2$ [17] and there is considerable scope for cross-slip to be the recovery mechanism for nucleating dynamic recrystallization. It may be noted that TX32 alloy will have poor hot ductility at temperatures higher than 500°C, since $Mg_2Ca$ at the grain boundaries forms a lower melting eutectic phase at about 516 °C [18] and leads to hot shortness.

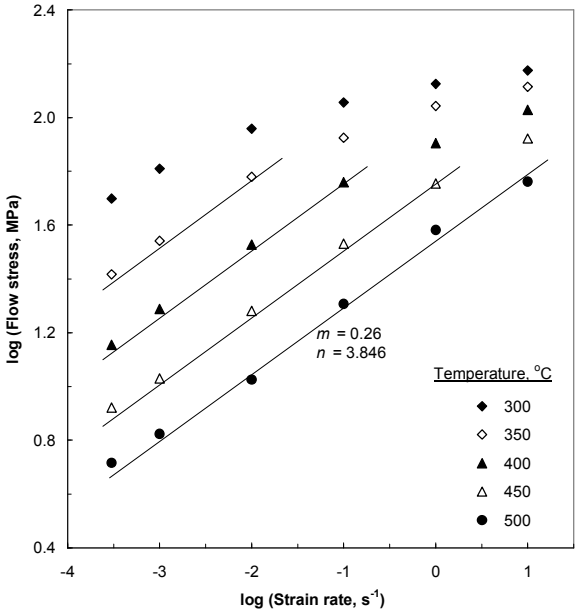


Fig. 5(a). Variation of flow stress (at a strain of 0.5) of TX32 alloy with strain rate on a log-log scale at different test temperatures.

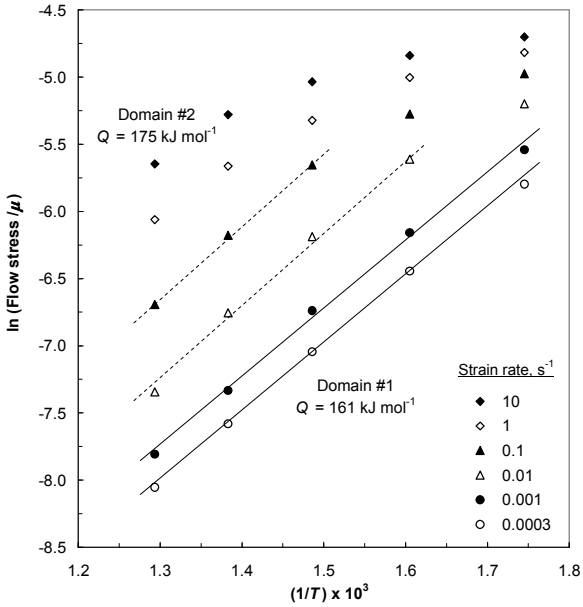


Fig. 5(b). Arrhenius plot showing the variation of normalized flow stress with inverse of temperature at different strain rates.

## Summary and Conclusions

The hot deformation behavior of Mg-3Sn-2Ca alloy in cast-homogenized condition has been studied using hot compression tests in the temperature range 300–500 °C and strain rate range 0.0003–10 s$^{-1}$. The flow stress data have been analyzed using processing map and kinetic analysis. The following conclusions are drawn from this investigation.

(1) At strain rates higher than 0.01 s$^{-1}$, the stress-strain curves exhibited flow softening behavior while at lower strain rates, near steady-state flow has been observed.

(2) The processing maps exhibited two domains: (1) 300–420 °C and 0.0003–0.003 s$^{-1}$, and (2) 420–500 °C and 0.003–1.0 s$^{-1}$, the latter one being suitable for industrial hot working of the alloy.

(3) Kinetic analysis in the two domains yielded values of apparent activation energy values of 161 and 175 kJ/mole respectively, which are higher than that for lattice self diffusion in Mg.

(4) The higher apparent activation energy values are attributed to the generation of back stress by the large volume fraction of CaMgSn intermetallic particles in the matrix.

(5) The presence of $Mg_2Ca$ precipitates at the grain boundaries is beneficial at slow strain rates but at higher strain rates they prevent grain-boundary self-diffusion and cause hot shortness at temperatures higher than 500 °C.

(6) The processing map has revealed a wide regime of flow instability at lower temperatures and higher strain rates, which has to be avoided in hot working of the alloy.

**Acknowledgement**

This work was supported by a grant (Project #115108) from the Research Grants Council of the Hong Kong Special Administrative Region, China.

**References**

[1] T. Abu Leil, K.P. Rao, N. Hort, K.U. Kainer, in: *Magnesium Technology 2006*, edited by A.A. Luo, N.R. Neelameggham and R.S. Beals, TMS (The Minerals, Metals & Materials Society (2006), p.281.
[2] T. Abu Leil, Y. Huang, H. Dieringa, N. Hort, K.U. Kainer, J. Bursik, Y. Jaraskova and K.P. Rao, Mater. Sci. Forum Vol.546-549 (2007), p.69.
[3] T. Abu Leil, K.P. Rao, N. Hort, Y. Huang, C. Blawert, H. Dieringa and K.U. Kainer, in: *Magnesium Technology 2007*, edited by R.S. Beals, A.A. Luo, N.R. Neelameggham, M.O. Pekguleryuz, TMS (The Minerals, Metals and Materials Society) (2007), p.257.
[4] N. Hort, K.P. Rao, T. Abu Leil, H. Dieringa, Y.V.R.K. Prasad , K.U. Kainer, in: *Magnesium Technology 2008*, edited by M. Pekguleryuz, E. Nyberg, R.S. Beals and N. Neerameggham, TMS (The Minerals, Metals and Materials Society) (2008) p.401.
[5] Y.V.R.K. Prasad, S. Sasidhara, *Hot working guide: A compendium of processing maps*, ASM International, Materials Park, Ohio (1997).
[6] Y.V.R.K. Prasad, T. Seshacharyulu, Inter. Mater. Rev. Vol. 43 (1998), p. 243.
[7] Y.V.R.K. Prasad, Jour. Mater. Eng. Perfor. Vol. 12 (2003), p. 638.
[8] H. Ziegler, in: *Progress in Solid Mechanics*, editors. I.N. Sneddon, R. Hill, John Wiley, New York, Vol.4 (1965), p. 91.
[9] J.J. Jonas, C.M. Sellars, W.J. McG. Tegart, Metall. Rev. Vol.14 (1969) p.1.
[10] Y.V.R.K. Prasad, K.P. Rao, Mater. Sci. Eng. A Vol.374 (2004) p. 335.
[11] H.J. Frost, M.F. Ashby, *Deformation-mechanism maps*, Pergamon Press, Oxford, (1982), p.44.
[12] Y.V.R.K. Prasad, K.P. Rao, Mater. Sci. Eng. A Vol. 487 (2008) p.316.
[13] Y.V.R.K. Prasad, K.P. Rao, Adv. Eng. Mater. Vol.9 (2007) p.558.
[14] Y.V.R.K. Prasad, K.P. Rao, N. Hort, K.U. Kainer, Mater. Letters Vol.62 (2008) p.4207.
[15] Y.V.R.K. Prasad, K.P. Rao, N. Hort, K.U. Kainer, Jour. Mater. Proc. Tech. Vol.201 (2008) p.359.
[16] Y.V.R.K. Prasad, K.P. Rao, N. Hort, K.U. Kainer, Mater. Sci. Eng. A Vol.502 (2009) p. 25.
[17] J.R. Morris, J. Scharff, K.M. Ho, D.E. Turner, Y.Y. Ye, M.H. Yoo, Philos. Mag. A Vol.76 (1997) p. 1065.
[18] A. Kozlov, M. Ohno, T. Abu Leil, N. Hort, K.U. Kainer, R. Schmid-Fetzer, Intermetallics, Vol.16 (2008) p.316.